Journal of Radiation Research, Vol. 61, No. 2, 2020, pp. 237–242
doi: 10.1093/jrr/rrz098
Advance Access Publication: 6 January 2020

Enhancement of membrane lipid peroxidation in lung cancer cells irradiated with monoenergetic X-rays at the K-shell resonance absorption peak of phosphorus

Hiroshi Maezawa[1,*], Hiroko P Indo[2], Noriko Usami[1], Hideyuki J Majima[2], Hiromu Ito[2], Ken Ohnishi[3] and Katsumi Kobayashi[1]

[1]Photon Factory, Institute of Material Science, High Energy Accelerator Research Organization, 1-1 Oho, Tsukuba, Ibaraki 305-0801, Japan
[2]Department of Oncology, Kagoshima University Graduate School of Medical and Dental Sciences, 8-35-1, Sakuragaoka, Kagoshima 890-8544, Japan
[3]Center for Humanities and Sciences, Ibaraki Prefectural University of Health Sciences, 4669-2 Oaza-ami, Ami, Inashiki, Ibaraki 300-0394, Japan
*Corresponding Author. Photon Factory, Institute of Material Science, High Energy Accelerator Research Organization, 1-1 Oho, Tsukuba, Ibaraki 305-0801, Japan. Tel: +81-029-864-5602; FAX: +81-029-864-3202; E-mail: maezawa.hiroshi@tokushima-u.ac.jp
(Received 8 October 2019; revised 23 November 2019; editorial decision 8 December 2019)

ABSTRACT

The aim of this study was to determine whether membrane lipid peroxidation in mammalian cells is enhanced by X-ray irradiation at the K-shell resonance absorption peak of phosphorus. A549 and wild-type *p53*-transfected H1299 (H1299/wt*p53*) cell lines derived from human lung carcinoma were irradiated with monoenergetic X-rays at 2.153 keV, the phosphorus K-shell resonance absorption peak, or those at 2.147 or 2.160 keV, which are off peaks. Immunofluorescence staining for 4-hydroxy-2-nonenal (HNE), a lipid peroxidation product, was used as marker for protein modification. In both cell lines, the HNE production was significantly enhanced after irradiation at 2.153 keV compared to sham-irradiation. The enhancement (E) was calculated as the ratio of the fluorescence intensity of irradiated cells to that of sham-irradiated cells. In both the cell lines, $E_{2.153}$ was significantly larger than $E_{2.147}$ and no significant difference between $E_{2.147}$ and $E_{2.160}$ was observed. The extra enhancement at 2.153 keV was possibly caused by energy transition within the phosphorus K-shell resonance absorption. Our results indicate that membrane lipid peroxidation in cells is enhanced by the Auger effect after irradiation at the K-shell resonance absorption peak of phosphorus rather than by the photoelectric effect of the constituent atoms in the membrane lipid at 2.147 keV.

Keywords: phosphorus K-shell absorption; Auger effect; lipid peroxidation; HNE; lung carcinoma cells

INTRODUCTION

Radiation-induced biological effects depend on the sites and the number of ionization events in an organism. The Auger effect in radioactive isotopes causes the release of multiple electrons from atomic orbits. The released electrons can ionize neighboring molecules by depositing sufficient energy [1–3]. The Auger effect can be induced after the photoelectric effect by X-ray-photon absorption within the K- and L-shell orbits of specific atoms in organisms [4–6]. Yokoya and Ito have reviewed photon-induced Auger effects of bromine, phosphorus, iodine and platinum atoms in biological entities such as nucleotides, DNA, bacteria, yeast and mammalian cells [7].

Phosphorus atoms are important constituents of DNA and the membrane lipid bilayer in cells. Kobayashi *et al.* have shown that inactivation and gene conversion of diploid yeast cells were enhanced by X-rays with energy of the K-shell resonance absorption peak of phosphorus (2.153 keV) compared to that of the off peaks (2.147 and 2.160 keV) [8]. Furthermore, lethality, mutagenesis, chromosome aberration and DNA double-strand breaks of cultured mammalian cells and irreparable DNA lesions in yeast cells were induced more efficiently at 2.153 keV than at off-peak energy [9–12].

Conventional X-rays and other ionizing radiations induce lipid peroxidation and fragmentation of cellular polyunsaturated fatty acids, resulting in the formation of malondialdehyde and 4-hydroxy-2-nonenal (HNE) [13–16]. Motoori *et al.* demonstrated that HNE level increased in HLE, a human hepatocellular carcinoma cell line, 2 h after irradiation with 200 kVp X-rays (15 Gy), a process suppressed by the overexpression of manganese-superoxide dismutase (Mn-SOD) [17]. Yet, the number of studies investigating membrane damage induced by K-shell photoionization of phosphorus is limited. No significant difference in membrane permeability to a test molecule,

p-nitrophenyl-α-D-glucopyranoside, was observed in yeast cells irradiated with and without phosphorus K-shell resonance absorption [8]. Therefore, whether the Auger effect causes oxidative damage to membranes in a cell remains unclear.

In this study, we aimed to determine whether membrane lipid peroxidation in mammalian cells is enhanced by X-ray irradiation at the K-shell resonance absorption peak of phosphorus. We investigated HNE production in human lung carcinoma cells irradiated with the energy of the phosphorus K-absorption peak. Our results revealed that compared to off-peak X-rays, X-rays with an energy peak at 2.153 keV efficiently generated membrane lipid peroxidation in cells.

MATERIALS AND METHODS

Antibodies

The mouse monoclonal antibody against HNE was purchased from the Japan Institute for the Control of Aging (Shizuoka, Japan). The Alexa Fluor 488-conjugated goat anti-mouse IgG(H + L) secondary antibody was obtained from Thermo Fisher Scientific Inc. (MA, USA).

Cells and preparation for sample irradiation

Human lung carcinoma cell lines, A549 (RCB0098, RIKEN Bio Resource Center, Ibaraki, Japan) and H1299/wt*p53* (H1299 cells transfected with pC53-SN3 containing wild type (wt) *p53* [18]), were used in this study. Both cell lines were chosen based on preliminary results, which indicated that they have lower activity of Mn-SOD compared to H1299 cells. We anticipated that HNE could be produced significantly by K-shell absorption of monoenergetic X-rays in phosphorus in both cell lines. The cells were cultured in Dulbecco's modified Eagle medium (Sigma-Aldrich Japan K.K., Tokyo, Japan) supplemented with 10% fetal bovine serum (GE Healthcare Life Sciences, PA, USA) and antibiotics (penicillin 50 units/ml and streptomycin 50 μg/ml, GIBCO, NY, USA) at 37°C in a humidified atmosphere of 5% CO_2. The H1299/wt*p53* cells were maintained in the presence of 350 μg/ml G418 (Roche Diagnostics, IN, USA). The cells were plated in a monolayer on glass-bottom dishes (35 mm, MatTek Co., MA, USA) 1 day before irradiation.

Irradiation with monoenergetic X-rays

Irradiation with monoenergetic X-rays was performed using beam-line BL-27A at the Photon Factory Synchrotron Storage Ring (2.5 GeV), High Energy Accelerator Research Organization (Tsukuba, Japan), as previously described by Konishi *et al.* [19]. A monoenergetic beam was generated using a monochromator (energy resolution: $\Delta E/E \approx 10^{-3}$) and emitted in the atmosphere in a fixed horizontal direction (y). The cross-section of the beam was 6.1 (x: horizontal) mm × 3.0 (z: vertical) mm. The energies of the X-rays used for irradiation (2.147, 2.153 and 2.160 keV) were selected using the absorption spectrum of calf thymus DNA film (1 mg/cm^2) [8].

The cell-loaded dish was mounted on a scanning stage and moved in the x- and z-direction according to a program for uniform irradiation of cells [20]. The exposure rate was measured using a parallel plate free-air ionization chamber set on the scanning stage [12, 20]. Typical exposure time per sample was about 0.9 min for 0.516 C/kg of exposure.

Estimation of dose from exposure

The dose (D_c [Gy]) of monoenergetic X-rays was calculated using the following equation under several assumptions:

$$D_c = X_{ex}F = X_{ex}W_h\{(\mu_{en}/\rho)_c/(\mu_{en}/\rho)_{air}\}A_f$$
$$= X_{ex}W_h\{\sum R_i(\mu_{en}/\rho)_i/(\mu_{en}/\rho)_{air}\}A_f,$$

where X_{ex} is exposure; F is exposure-dose conversion factor; W_h is 33.5 J/C, which is the mean energy required to create an ion pair in humid (around 40%) room air [21]; R_i is the relative mass abundance of ith element in total soft tissue model [22]; $(\mu_{en}/\rho)_c$, $(\mu_{en}/\rho)_{air}$ and $(\mu_{en}/\rho)_i$ are the mass energy absorption coefficient of cells, air and ith element, respectively, and A_f is the dose attenuation factor of X-rays in cells [11]. A_f is calculated as $(1/t)[1/\{(\mu/\rho)_c\rho\}][1\text{- }\exp\{(\mu/\rho)_c\rho t\}]$, where t is assumed to be 6.5 μm as the thickness of lung carcinoma cells [23]; $(\mu/\rho)_c$ is the mass attenuation coefficient of cells and ρ is assumed to be 1 g/cm^3 as the density of cells. For air and elements, (μ_{en}/ρ) and (μ/ρ) at selected energy were estimated using data tabled by Seltzer and Hubbell [24]. For phosphorus, $(\mu_{en}/\rho)_{2.153}$ at 2.153 keV was estimated using the ratio (= 4.9) of $\{(\mu_{en}/\rho)_{2.153-}(\mu_{en}/\rho)_{2.147}\}$ to $\{(\mu_{en}/\rho)_{2.160-}(\mu_{en}/\rho)_{2.147}\}$ and $(\mu/\rho)_{2.153}$ using a similar equation [8]. The $(\mu_{en}/\rho)_c$ [m^2/kg] was calculated as 42.7, 43.6 and 42.2 at 2.147, 2.153 and 2.160 keV, respectively.

Immunofluorescence assay for HNE

Immunofluorescence staining with an anti-HNE monoclonal antibody was performed according to the procedure of Indo *et al.* [16]. Briefly, immediately after irradiation, cells were incubated in fresh medium for 2 h at 37°C. Cells were fixed for 30 min at room temperature using HistoChoice® MB Tissue Fixative (Amresco Inc., MD, USA), instead of formaldehyde. The following permeabilization was done with a 5% acetic acid/95% ethanol mixture for 10 min. The specimens were blocked with 1% bovine serum albumin in Dulbecco's phosphate-buffered saline for 30 min and then incubated with anti-HNE antibody for 1 h at room temperature. After rinsing, the cells were incubated with the secondary antibody for 1 h. Images of cellular HNE fluorescence were captured using a confocal laser microscope scanner unit (excitation at 488 nm; fluorescence transmitted 515-nm barrier filter; Yokogawa Electric Co., Tokyo, Japan), which was attached to an inverted microscope (Olympus Optical Co., Tokyo, Japan) with an objective lens and a color-chilled CCD camera (Hamamatsu Photonics K.K., Shizuoka, Japan). The intensity and the exposure time of the excitation laser were set at 500 μW and 4 s, respectively. Three dishes and three random fields per dish were used to obtain >50 images of cells from each group. The values of the average fluorescence intensity/cell were obtained using IPLab Spectrum version 3.0 software (Scananalystics Inc., Fairfax, VA) with some modification of the program by one of the authors (H.J.M).

Statistical analysis

Data are presented as mean and standard deviation. Statistical analysis was performed using the Statcel4 software (OMS Co., Saitama, Japan) and Excel (Microsoft Co., WC, USA) on Macintosh OSX (Apple Computer Inc., CA, USA) and applying one-way analysis of variance (ANOVA), followed by Scheffe's F test. P values <0.05 were considered statistically significant.

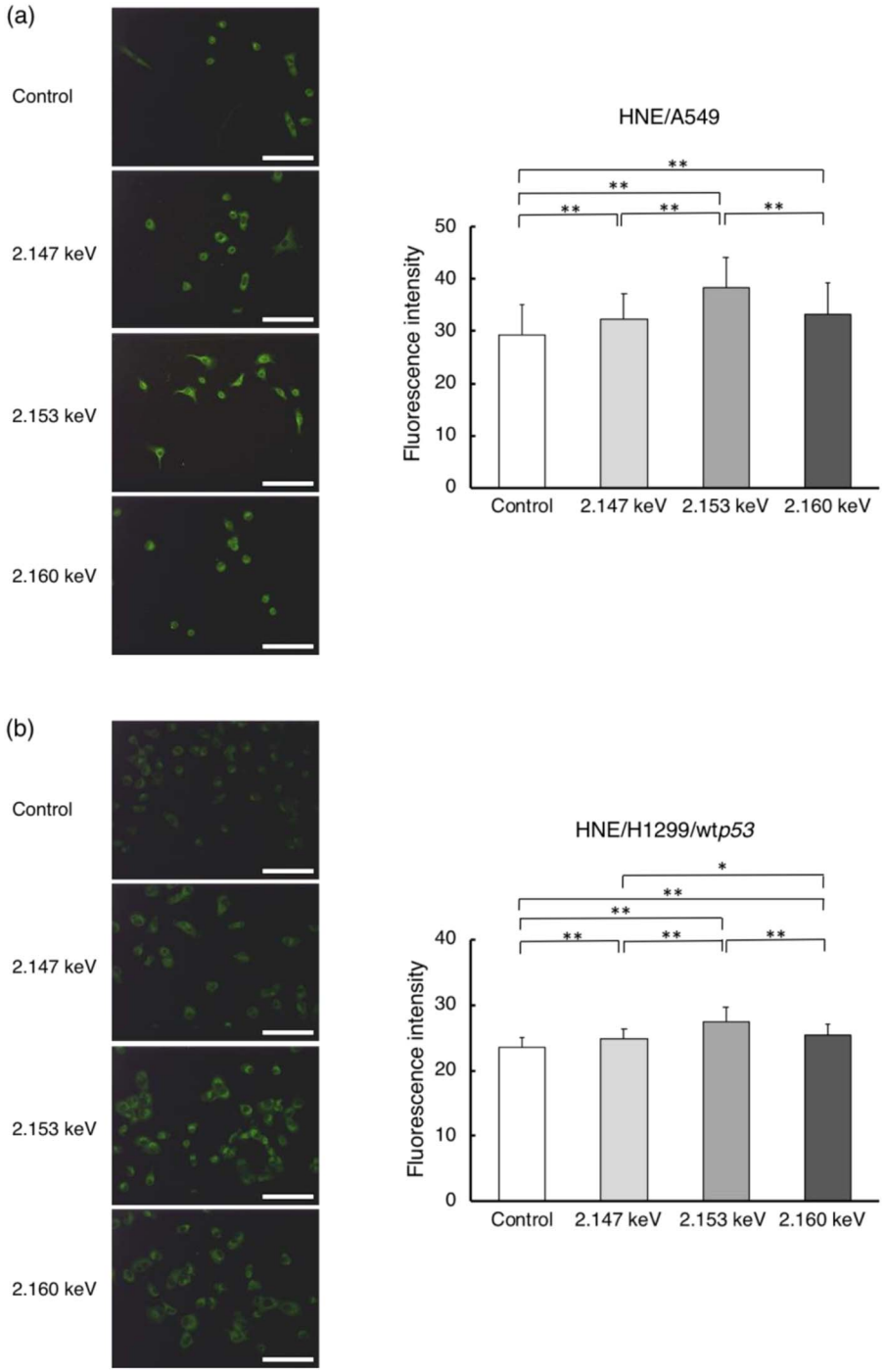

Fig. 1. Intracellular HNE production in (a) A549 and (b) H1299/wt*p53* cells 2 h post-irradiation (15.3 Gy). Representative immunofluorescence images (green, ×20 magnification) and fluorescence intensity per cell are shown for irradiated and sham-irradiated control cells. Values represent the mean ± standard deviation. $^{*}P < 0.05$, $^{**}P < 0.01$; Sheffe's F tests ($n > 163$ for A549, $n > 191$ for H1299/wt*p53*). Scale bar = 50 μm.

RESULTS AND DISCUSSION

In both A549 and H1299/wt*p53* cell lines, the HNE fluorescence intensity was significantly higher after irradiation at 15.3 Gy compared to control sham-irradiation (Fig. 1). In addition, the fluorescence intensity at 2.153 keV was significantly higher than that at 2.147 or 2.160 keV. We published the mitochondrial event caused by

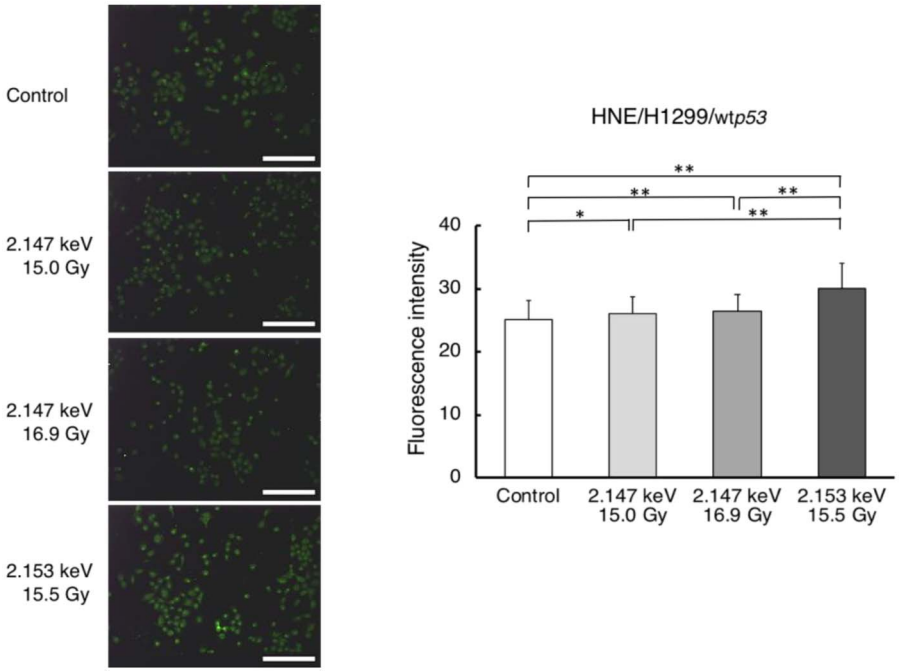

Fig. 2. Dose-independent generation of HNE in H1299/wt*p53* cells irradiated with 2.147 keV radiation. Cells were irradiated with 15.0 Gy and 16.9 Gy at 2.147 keV and with 15.5 Gy at 2.153 keV. Two hours after irradiation, the cells were fixed and immunofluorescence staining with an anti-HNE antibody was performed. Representative immunofluorescence images (green, ×10 magnification) and fluorescence intensity per cell are shown. Values represent the mean ± standard deviation. $^{*}P < 0.05$, $^{**}P < 0.01$; Sheffe's F tests ($n > 190$). Scale bar = 100 μm.

Table 1. Enhancement of the fluorescence intensity corresponded to HNE production in A549 and H1299/wt*p53* cells after monoenergetic X-ray irradiation

Cells	X-ray energy (keV)	Dose[a] (Gy)	Enhancement[a,b]
A549			
	2.147	15.2 ± 0.3	1.07 ± 0.03
	2.153	15.4 ± 0.1	1.20 ± 0.08*
	2.160	15.2 ± 0.1	1.10 ± 0.03
H1299/wt*p53*			
	2.147	15.3 ± 0.6	1.05 ± 0.05
	2.153	15.6 ± 0.4	1.17 ± 0.04*,**
	2.160	15.4 ± 0.4	1.05 ± 0.06

[a]Values represent the mean ± standard deviation obtained from four independent experiments.
[b]Enhancement = (fluorescence intensity of irradiated cells)/(fluorescence intensity of sham-irradiated cells).
* $P < 0.05$ versus 2.147 keV, ** $P < 0.05$ versus 2.160 keV, Scheffe's F test for three irradiation groups.

X-irradiation for the first time in 2001 [17] and proved that besides nuclear events, mitochondrial reactive oxygen species (ROS)-related events caused apoptosis. To see the most visible events, we chose 18.8 Gy X-irradiation to understand the role of Mn-SOD in the mitochondrial ROS-caused HNE and apoptosis events [16]. In this paper, we proved that ROS and HNE are produced in mitochondria. This time, we assumed the same events will occur as a result of Auger events in phosphorus irradiation. The purpose of this study is to show that the same mitochondrial ROS-caused HNE is visible in the Auger events of phosphorus irradiation, and we chose the most visible 15 Gy phosphorus irradiation. We also found that HNE production is visible in the mitochondrial region in this study also.

The enhancement (E) was calculated as the ratio of the fluorescence intensity of the irradiated cells to that of the control. For A549 cells, $E_{2.153}$ was significantly larger than $E_{2.147}$, but not $E_{2.160}$ (Table 1). For H1299/wt*p53* cells, the $E_{2.153}$ was significantly larger than $E_{2.147}$ and $E_{2.160}$. The $E_{2.153}$ was not significantly different between A549 and H1299/wt*p53* cells. No significant difference between $E_{2.147}$ and $E_{2.160}$ was observed for both cell lines. The extra enhancement ($E_{2.153}-E_{2.147}$) was about 0.1 in both cell lines. These results indicate that compared to irradiation at 2.147 keV, energy of 2.153 keV enhanced the production of HNE in the membrane.

An experiment was performed to confirm the effect of a slight dose difference between 2.153 keV and 2.147 keV on HNE production. The fluorescence intensities upon exposure to 16.9 Gy and 15.0 Gy at 2.147 keV did not significantly differ, but irradiation with 15.5 Gy at 2.153 keV resulted in higher fluorescence intensity (Fig. 2). The fluorescence intensity in Fig. 2 was significantly different from that in Fig. 1, but no significant difference of $E_{2.153}$ was observed between both figures. This suggests that the production of HNE was more efficient in terms of dose at 2.153 keV compared to that at 2.147 keV.

Superoxide generated by the electron transport chain in the mitochondrial membrane can cause lipid peroxidation [25–27]. The generation of superoxide from mitochondria increases upon conventional X-ray irradiation [17, 28]. The electrons emitted after X-ray-photon K-shell resonance absorption of phosphorus may also induce disorder of mitochondrial function in cells. In addition, the Auger effect of phosphorus produces multi-charged cationic phosphorus. The rearrangement of charges may cause bond breakage in phospholipids, resulting in mitochondrial disorder [9]. An increase in mitochondrial disorder after irradiation at 2.153 keV occurred in both A549 and H1299/wt*p53* cells.

Further studies are needed to clarify the dependence of the induction of lipid peroxidation by phosphorus Auger effect on the dose and the activity of Mn-SOD. In conclusion, we anticipate that HNE production at 2.153 keV was partially caused by mechanisms that differ from those at 2.147 keV. The Auger effect after irradiation at the energy of the K-shell resonance absorption peak of phosphorus may induce membrane lipid peroxidation in cells.

ACKNOWLEDGMENTS

We are grateful to Dr. A. Yokoya (QST) for critical reading of the manuscript. This work was performed under the approval of the Photon Factory Program Advisory Committee (Proposal No. 2012G746, 2015PF28).

FUNDING

None.

REFERENCES

1. Kassis AI, Adelstein SJ, Haydock C et al. Lethality of Auger electrons from the decay of bromine-77 in the DNA of mammalian cells. *Radiat Res* 1982;90:362–73.
2. Pomplun E, Booz J, Charlton DE. A Monte Carlo simulation of Auger cascades. *Radiat Res* 1987;111:533–52.
3. Sastry KSR. Biological effects of the Auger emitter iodine-125: A review. Report no.1 of AAPM nuclear medicine task group no.6. *Med Phys* 1992;19:1361–70.
4. Halpern A, Mutze B. Irradiation of micro-organisms with monoenergetic X-rays; biological consequences of the Auger effect. *Int J Radiat Biol* 1978;34:67–72.
5. Booz J. Microdosimetric basis of individualized cancer radiotherapy by radionuclides including Auger effect and the photon activation approach. *Strahlenther* 1984;160:745–54.
6. Fairchild RG, Bond VP. Photon activation therapy. *Strahlenther* 1984;160:758–63.
7. Yokoya A, Ito T. Photon-induced Auger effect in biological systems: A review. *Int J Radiat Biol* 2017;93:743–56.
8. Kobayashi K, Hieda K, Maezawa H et al. Effects of K-shell X-ray absorption of intracellular phosphorus on yeast cells. *Int J Radiat Biol* 1991;59:643–50.
9. Watanabe M, Suzuki M, Watanabe K et al. Mutagenic and transforming effects of soft-X-rays with resonance energy of phosphorus K-absorption edge. *Int J Radiat Biol* 1992;61:161–8.
10. Saigusa S, Ejima Y, Kobayashi K et al. Induction of chromosome aberrations by monochromatic X-rays with resonance energy of phosphorus K-shell absorption edge. *Int J Radiat Biol* 1992;61:785–90.
11. Tomita M, Maeda M, Usami N et al. Enhancement of DNA double-strand break induction and cell killing by K-shell absorption of phosphorus in human cell lines. *Int J Radiat Biol* 2016;92:724–32.
12. Usami N, Yokoya A, Ishizaka S et al. Reparability of lethal lesions produced by phosphorus photoabsorption in yeast cells. *J Radiat Res* 2001;42:317–31.
13. Reisz JA, Bansal N, Qian J et al. Effects of ionizing radiation on biological molecules- mechanisms of damage and emerging methods of detection. *Antioxid Redox Signal* 2014;21:260–92.
14. Wills ED, Wilkinson AE. Release of enzymes from lysosomes by irradiation and the relation of lipid peroxide formation to enzyme release. *Biochem J* 1966;99:657–66.
15. Dittmann K, Mayer C, Kehlbach R. Radiation-induced lipid peroxidation activates src kinase and triggers nuclear EGFR transport. *Radiat Oncol* 2009;92:379–82.
16. Indo HP, Inanami O, Koumura T et al. Roles of mitochondria-generated reactive oxygen species on X-ray-induced apoptosis in a human hepatocellular carcinoma cell line, HLE. *Free Radical Research* 2012;46:1029–43.
17. Motoori S, Majima HJ, Ebara M et al. Overexpression of mitochondrial manganese superoxide dismutase protects against radiation-induced cell death in the human hepatocellular carcinoma cell. *Cancer Res* 2001;61:5382–8.
18. Ohnishi K, Scuric Z, Schiestl RH et al. siRNA targeting *NBS1* or *XIAP* increases radiation sensitivity of human cancer cells independent of *TP53* status. *Radiat Res* 2006;166:454–62.
19. Konishi H, Yokoya A, Shiwaku H et al. Synchrotron radiation beamline to study radioactive materials at the Photon Factory. *Nucl Instrum Methods Phys Res Sec A* 1996;372:322–32.
20. Kobayashi K, Hieda K, Maezawa H et al. Monochromatic X-ray irradiation system (0.08-0.4 nm) for radiation biology studies using synchrotron radiation at the Photon Factory. *J Radiat Res* 1987;28:243–53.
21. International Commission on Radiation Units and Measurements. Key data for ionizing-radiation dosimetry: Measurement standards and applications. *J ICRU* 2014;14:31–47.
22. International Commission on Radiological Protection. *Report of the task group on reference man. ICRP Publication 23*. Oxford: Pergamon Press, 1975.
23. Boudreault F, Grygorczyk R. Evaluation of rapid volume changes of substrate-adherent cells by conventional microscopy 3D imaging. *J Microscopy* 2004;215:302–12.
24. Seltzer SM, Hubbell JH. Tables and graphs of photon mass attenuation coefficients and mass energy-absorption coefficients for photon energies 1 keV to 20 MeV for elements z = 1 to 92 and some dosimetric materials. In: Maekoshi H (ed). *Data Book of Photon Attenuation Coefficients*. Kyoto: Japanese Society of Radiological Technology, 1995, 9–172.

25. Majima HJ, Indo HP, Tomita K et al. Intracellular oxidative stress caused by ionizing radiation. In: Singh K (ed). *Oxidative Stress, Disease and Cancer*. London: Imperial College Press, 2006, 61–83.
26. Majima HJ, Indo HP, Suenaga S et al. Mitochondria as source of free radicals. In: Naito Y, Suematsu M, Yoshikawa T (eds). *Free Radical Biology in Digestive Diseases*. Basel: Karger, 2011, 12–22.
27. Indo HP, Yen HC, Nakanishi I et al. A mitochondrial superoxide theory for oxidative stress diseases and aging. *J Clin Biochem Nutr* 2015;56:1–7.
28. Ogura A, Oowada S, Kon Y et al. Redox regulation in radiation-induced cytochrome c release from mitochondria of human lung carcinoma A549 cells. *Cancer Lett* 2009;277:64–71.